



Shelf-to-basin iron shuttling enhances vivianite formation in deep Baltic Sea sediments



Daniel C. Reed^{a,*}, Bo G. Gustafsson^b, Caroline P. Slomp^a

^a Department of Earth Sciences (Geochemistry), Faculty of Geosciences, Utrecht University, The Netherlands

^b Baltic Nest Institute, Stockholm University, SE-106 91 Stockholm, Sweden

ARTICLE INFO

Article history:

Received 27 May 2015

Received in revised form 20 November 2015

Accepted 23 November 2015

Available online 10 December 2015

Editor: H. Stoll

Keywords:

iron

phosphorus

eutrophication

sediment geochemistry

reactive-transport modelling

Baltic Sea

ABSTRACT

Coastal hypoxia is a growing and persistent problem largely attributable to enhanced terrestrial nutrient (i.e., nitrogen and phosphorus) loading. Recent studies suggest phosphorus removal through burial of iron (II) phosphates, putatively vivianite, plays an important role in nutrient cycling in the Baltic Sea – the world's largest anthropogenic dead zone – yet the dynamics of iron (II) phosphate formation are poorly constrained. To address this, a reactive-transport model was used to reconstruct the diagenetic and depositional history of sediments in the Fårö basin, a deep anoxic and sulphidic region of the Baltic Sea where iron (II) phosphates have been observed. Simulations demonstrate that transport of iron from shelf sediments to deep basins enhances vivianite formation while sulphide concentrations are low, but that pyrite forms preferentially over vivianite when sulphate reduction intensifies due to elevated organic loading. Episodic reoxygenation events, associated with major inflows of oxic waters, encourage the retention of iron oxyhydroxides and iron-bound phosphorus in sediments, increasing vivianite precipitation as a result. Results suggest that artificial reoxygenation of the Baltic Sea bottom waters could sequester up to 3% of the annual external phosphorus loads as iron (II) phosphates, but this is negligible when compared to potential internal phosphorus loads due to dissolution of iron oxyhydroxides when low oxygen conditions prevail. Thus, enhancing vivianite formation through artificial reoxygenation of deep waters is not a viable engineering solution to eutrophication in the Baltic Sea. Finally, simulations suggest that regions with limited sulphate reduction and hypoxic intervals, such as eutrophic estuaries, could act as important phosphorus sinks by sequestering vivianite. This could potentially alleviate eutrophication in shelf and slope environments.

© 2015 Elsevier B.V. All rights reserved.

1. Introduction

Hypoxic bottom waters ($[O_2] < 2 \text{ mg L}^{-1}$) associated with eutrophication are a serious and persistent problem in coastal regions throughout the oceans (Rabalais et al., 2014). Oxygen-depletion has a profound impact on marine biogeochemistry, perturbing large-scale nutrient cycling (Savchuk, 2010), reducing biodiversity (Levin et al., 2009), and altering ecosystem function (Villnäs et al., 2012). Hypoxia results from an excess of nutrients in surface waters stimulating primary production and enhancing export of organic matter to deeper waters, where it undergoes microbially-mediated remineralisation. If oxygen is not replenished via transport mechanisms, this increase in oxygen uptake by microbes causes deep waters to become hypoxic.

Reported occurrences of hypoxia in the coastal ocean have increased significantly in recent decades providing impetus for studying the biogeochemistry of hypoxic systems as they develop, particularly with regards to nutrient dynamics (Diaz and Rosenberg, 2008). Phosphorus (P) is a key nutrient in marine environments as it is essential for life and, unlike nitrogen, cannot be fixed from the atmosphere. The only long-term sink for phosphorus in the oceans is burial in sediments, in the form of authigenic and detrital minerals as well as organic matter (Ruttenberg, 2003). Retention of phosphorus in sediments, however, exhibits a marked redox dependency: under oxygen-depleted conditions organic phosphorus is remineralised faster relative to organic carbon and phosphorus-bearing iron oxyhydroxides undergo dissolution (Mortimer, 1941; Ingall et al., 1993; Ingall and Jahnke, 1994; Slomp et al., 1996, 2002). These mechanisms represent potential positive feedbacks in hypoxic systems, as an enhanced efflux of phosphate from the seafloor may fuel elevated productivity in overlying waters. Therefore, as low oxygen regions of the coastal ocean expand throughout the world, it is increasingly important to

* Corresponding author. Current address: School of the Environment, Washington State University, Vancouver, WA, USA. Tel.: +1 (734) 358 0608.

E-mail address: dan.reed@wsu.edu (D.C. Reed).

have a comprehensive and quantitatively coherent understanding of sedimentary phosphorus cycling if remediation efforts are to be successful.

Of the regions that have become hypoxic due to human activities, the one in the Baltic Sea is the largest in the world's oceans (Diaz and Rosenberg, 2008). In the pelagic Baltic Sea, phosphorus co-limits primary production and it is the principal limiting nutrient in other regions, such as the Gulf of Finland (Moisander et al., 2003). Whereas phosphorus removal is dominated by burial of organic matter in much of the Baltic Sea (Mort et al., 2010), recent observations suggest that burial of reduced iron-phosphorus minerals – likely vivianite ($\text{Fe}_3(\text{PO}_4)_2 \cdot 8\text{H}_2\text{O}$) – may also represent a significant sink for phosphorus (Jilbert and Slomp, 2013a; Slomp et al., 2013). While precipitation of vivianite is usually associated with high concentrations of pore water iron in the absence of hydrogen sulphide, such as below the sulphate–methane transition zone (e.g., März et al., 2008; Slomp et al., 2013; Rutteneberg, 2003), vivianite formation has also been reported within the sulphate–methane transition zone in Baltic Sea sediments where pore waters are undersaturated with respect to vivianite, suggesting an alternative formation mechanism (Jilbert and Slomp, 2013a). Knowledge of the dynamics of vivianite formation remains poor, however, in spite of the potentially important role as a phosphorus sink in brackish coastal systems (Egger et al., 2015a), freshwater lakes (Rothe et al., 2014), and rivers (Hearn et al., 1983).

With this in mind, here we explore vivianite's role in benthic phosphorus cycling using a comprehensive diagenetic model. The model is employed to interpret solid phase and pore water data from F80, a site located in a deep basin in the Baltic Sea where reduced iron-phosphate precipitation has been previously observed (Jilbert and Slomp, 2013a). Over the past century, this region has undergone shifts in environmental conditions (e.g., bottom water redox conditions (Carstensen et al., 2014b), organic loading (Gustafsson et al., 2012)) in response to eutrophication. Initially, elevated nutrient loading led to enhanced organic matter export from surface waters to underlying sediments (Gustafsson et al., 2012). We postulate that this resulted in a shoaling in the oxygen penetration depth and an increase in dissimilatory iron reduction in coastal sediments. Prior to the increase in organic loading, iron reduction was incomplete resulting in the burial of iron oxyhydroxides, like in the Bothnian Sea, which serves as an analogue for the Baltic Sea prior to eutrophication. As a result, there was an elevated efflux of dissolved iron (Fe^{2+}) into the water column where iron oxyhydroxides were precipitated and then transported down slope to be deposited in deeper sediments. This diagenetic reduction of iron oxyhydroxides and subsequent syngenetic reprecipitation of the released dissolved iron may have occurred numerous times, gradually moving iron deeper into the basin. In addition to oxyhydroxides, iron may also be transported in solution as Fe^{2+} in anoxic waters, whereas iron may precipitate as pyrite or other sulphides in euxinic (i.e., anoxic and sulphidic) waters (Raiswell and Canfield, 2012). This phenomenon, often termed the *shelf-to-basin iron shuttle*, ultimately results in an iron enrichment in deep sediments (Canfield et al., 1996) and has previously been shown to be active in this region of the Baltic Sea (Scholz et al., 2013). These sediments also become enriched in organic matter due to elevated productivity associated with eutrophic surface waters, which in turn leads to a decline in redox conditions due to higher rates of microbially-mediated degradation of organic compounds. Bottom water oxygen concentrations are consequently drawn down to the point of hypoxia or even anoxia. When such deep basins become euxinic, iron is sequestered in sediments as iron sulphides (e.g., pyrite) and buried (Bernier, 1984). Sediments subject to lower depositional fluxes of iron are able to retain less sulphide and, therefore, overlying waters are more prone to euxinia (Diaz and Rosenberg, 2008).

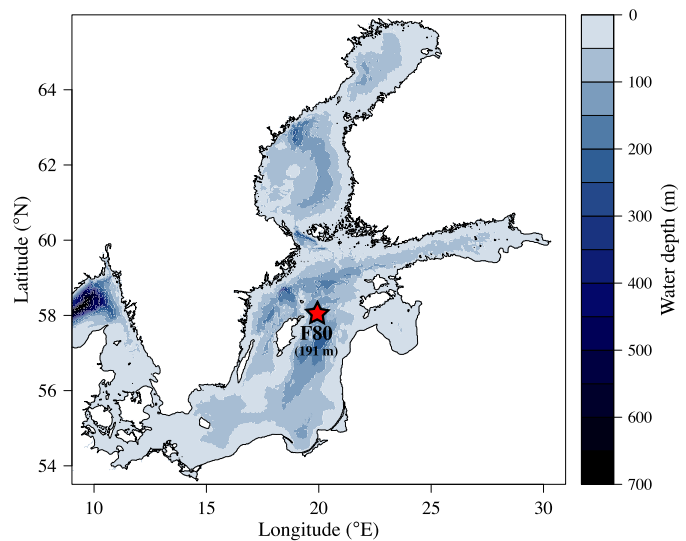


Fig. 1. Location of field site F80 within the Baltic Sea.

The simulations presented here are performed to test the hypothesis that fluctuations in the iron shuttle explain variations in diagenetic vivianite. The data set from F80 lends itself well to the study of vivianite formation because microanalysis of epoxy resin-embedded sediments from this site has previously revealed the presence of reduced iron-phosphorus minerals, putatively vivianite (Jilbert and Slomp, 2013a). Analysis of these data through reactive-transport modelling allows environmental conditions over the past century to be reconstructed, providing insight into the development of euxinic bottom waters and its impact on biogeochemical dynamics. Initially, we reconstruct the conditions under which these sediments were deposited, from the early 20th century to present day, illuminating the evolution of euxinia in deep basins. Next, we establish how these geochemical transitions have altered phosphorus, iron, and sulphur dynamics, retention, and speciation in underlying sediments. In particular, we examine the role played by changes in iron deposition (i.e., the iron shuttle) and the feedbacks between phosphorus, iron, and sulphur cycling. Finally, we consider the impact of reoxygenation events on sedimentary phosphorus retention and the implications of our findings for phosphorus burial in eutrophic coastal systems.

2. Study site and data set

The Baltic Sea is a semi-enclosed brackish sea bounded by mainland Europe and the Scandinavian peninsula, connected to the North Sea via the Danish Straits. With an average depth of only 54 m, the Baltic Sea is relatively shallow, yet it is punctuated by several deep basins. Here, we focus on a field site in one such basin: F80 (19.8968E 58.0000N) located in the Färö basin of the Baltic Proper at a depth of 191 m (Fig. 1). Permanent salinity stratification restricts ventilation of the basin, which contributes towards oxygen-depleted bottom waters, although the Färö deep has been oxic and/or hypoxic for much of the past 4000 yrs (Jilbert and Slomp, 2013b). Since 1980, the bottom waters of the basin have been largely euxinic (Fig. 2). Nevertheless, episodic major inflow events, where dense oxic water from the North Sea is forced through the Danish Straits and sinks into deep basins, temporally alleviates euxinia by reoxygenating bottom waters (Fig. 2). The most recent of these major inflow events occurred in 1993, 2003 and 2014 (Mohrholz et al., 2015), although the latter inflow is not relevant to the period captured in our data set.

Hypoxia was largely confined to the deepest regions of the Baltic Sea in the early 20th century, but has since expanded

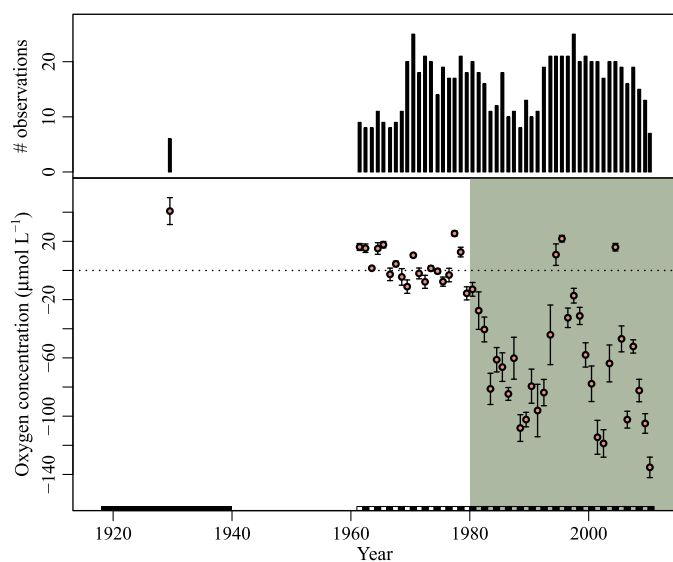


Fig. 2. Observations of oxygen concentrations at F80 over the late 20th and early 21st centuries. Error bars show the standard deviation in measurements and the shaded region shows the period assumed to be euxinic by the model. Negative oxygen concentrations represent hydrogen sulphide equivalents ($-2 \text{ mol O}_2 = 1 \text{ mol H}_2\text{S}$, Gustafsson et al., 2012). The bar along the horizontal axis shows the averaging interval, while the upper pane shows the number of observations within that interval. These data are taken from the Baltic Environmental Database at Stockholm University, Sweden.

from an area of 5000 km² to over 60,000 km² in just the Gotland and Bornholm basins alone (Carstensen et al., 2014a). The area of seafloor overlain by hypoxic bottom waters has exhibited marked variability on both seasonal and decadal time scales, however, meaning sediments are subject to redox fluctuations on a broad range of temporal scales. Previous studies have demonstrated the importance of variable redox conditions on sedimentary phosphorus sequestration chiefly due to two mechanisms (e.g., Reed et al., 2011a, 2011b; Kraal et al., 2010; Tsandev et al., 2012; Ingall et al., 1993; Slomp et al., 2002; Jilbert et al., 2011). First, a decline in bottom water oxygen attenuates remineralisation via aerobic respiration, leading to an increase in iron reduction. Low oxygen concentrations allow dissolved iron and iron-bound phosphorus released during iron reduction to escape into bottom waters rather than be reprecipitated within the sediment (Mortimer, 1941). This additional release of phosphorus augments the existing efflux, which may already be significant if iron oxyhydroxides are saturated with respect to phosphate (e.g., Sundby et al., 1992; Katsev et al., 2007). Second, the loss of oxygen – an important terminal electron acceptor – enhances the accumulation of organic matter and associated organic phosphorus in sediments. Nevertheless, organic phosphorus is remineralised faster than organic carbon under reducing conditions, which attenuates the long term retention of phosphorus in sediments (Ingall et al., 1993; Slomp et al., 2002; Jilbert et al., 2011). As these redox-sensitive processes occur on a broad range of time scales, the length of the low-oxygen episode is potentially important (cf. Reed et al., 2011b, 2011a). While these mechanisms and the benthic phosphorus cycle in general have been explored quantitatively using reactive-transport models (e.g., Reed et al., 2011b, 2011a; Dale et al., 2013; Katsev et al., 2007), the role of vivianite formation in marine sediments is yet to be explored, despite its inclusion in models of freshwater sediments (Katsev et al., 2006; Katsev and Dittrich, 2013).

Field station F80 provides an excellent opportunity for studying these processes, as the concentration of iron-phosphate has been observed to vary over the past 40 yrs at F80 in response to redox fluctuations and shifts in other environmental parameters

associated with eutrophication (Jilbert and Slomp, 2013a). To extricate and explore the influence that these environmental forcings have on diagenetic processes, especially those pertaining to iron and phosphorus dynamics, we adapt and apply a reactive-transport model to a data set from F80 (Jilbert and Slomp, 2013a), which comprises a comprehensive suite of sediment and pore water profiles extending to 32 cm depth, deposited over 43 yrs. Specifically, the model is calibrated using data for organic C and P, dissolved iron and manganese, methane, sulphate, ammonium, dissolved phosphate, and CDB-phosphorus (Figs. 5a, 6a, and 7a of Jilbert and Slomp, 2013a). CDB-phosphorus – denoted hereafter as Fe–P – is phosphorus extracted by the citrate–dithionite–bicarbonate step of the SEDEX sequential extraction procedure (Ruttenberg, 1992). The CDB step dissolves iron oxyhydroxides and, therefore, Fe–P is interpreted as phosphorus that is bound to these species. Nonetheless, pyrite (Slomp et al., 1996), iron monosulphide (Egger et al., 2015b) and vivianite (Nembrini et al., 1983) can also be extracted to some degree and, therefore, CDB iron and phosphorus represent composite signals of these species. In addition to these published data, we also drew on previously unpublished profiles from the same data set for porosity, CaCO₃, organic nitrogen, dissolved inorganic carbon, solid phase sulphur, and CDB-Fe. All data are from sediment cores that were recovered by means of a multicorer during two research cruises in May–June of 2009 and June–July of 2010 on the R/V Aranda and R/V Heincke, respectively. Analytical methods employed to produce these additional data are described by Jilbert (2011, porosity, organic N) and Mort et al. (2010, CaCO₃, organic N, solid phase S, CDB-Fe). Samples for dissolved inorganic carbon (DIC) analysis were collected in 5 ml headspace vials, poisoned with 10 μL of saturated HgCl₂ and subsequently analysed photometrically as described by Stoll et al. (2001). Finally, the age model presented for F80 by Jilbert and Slomp (2013b) has recently been revised by Lenz et al. (2015) and we use the updated version here. All additional data are included in the supplementary material (Table S11; Fig. S1).

3. Methods

3.1. Reactive-transport model

The diagenetic model employed here was developed by Reed et al. (2011b) and has been expanded to include pH-associated speciation using the *Direct Substitution Approach* (Hofmann et al., 2008), as well as a diffusive boundary layer (Boudreau, 1997, p. 182). The model is a conventional 1D multicomponent diagenetic model (Boudreau, 1996; Soetaert et al., 1996; Van Cappellen and Wang, 1996) that describes the vertical distribution and temporal evolution of chemical profiles subject to various reactions (see Supplementary Material) and transport processes, including burial due to sedimentation, steady-state compaction, and molecular diffusion (for solutes only). Bioturbation and bioirrigation are omitted from the model since F80 is naturally hypoxic, thus precluding the presence of benthic fauna. Porosity at F80 exhibits the familiar exponential form (Table S11) and is quantified by fitting the canonical porosity function to these data (Boudreau, 1997, p. 223). Similarly, tortuosity is described as a function of porosity using a standard expression (Boudreau, 1997, p. 132).

3.2. Vivianite kinetics

In addition to the suite of reactions used by Reed et al. (2011b), the rate of vivianite precipitation (R_{viv}) is modelled by means of Michaelis–Menten kinetics for dissolved iron and phosphate, ac-

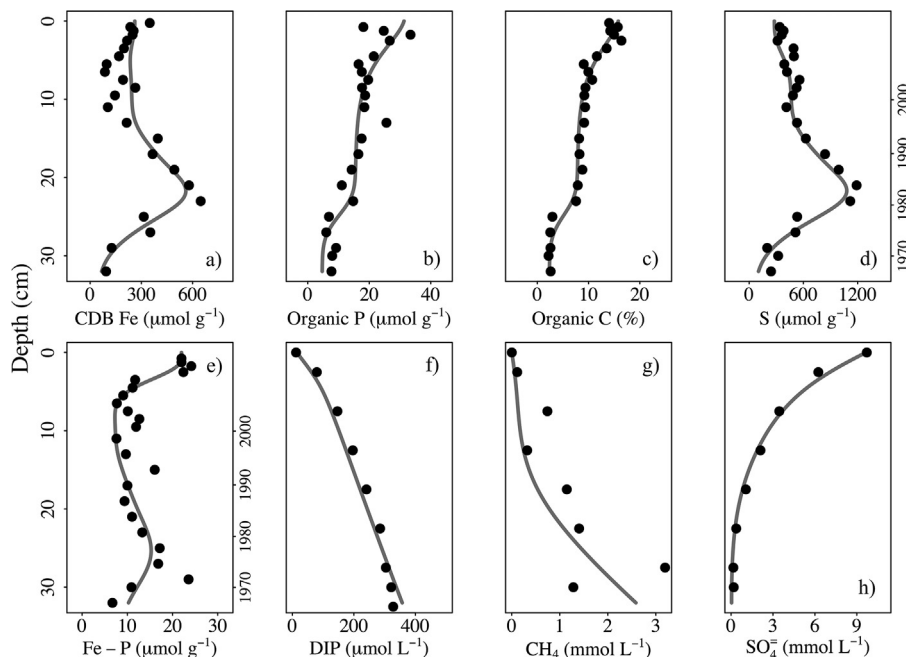


Fig. 3. Profiles of relevant chemical species: a) citrate–dithionite–bicarbonate extracted iron (CDB Fe – in the model, assumed to be a composite of amorphous and well-crystalline iron oxyhydroxides, vivianite, FeS and FeS₂), b) organic phosphorus, c) organic carbon, d) solid phase sulphur, e) iron-bound phosphorus (Fe–P – in the model, a composite of vivianite and phosphorus bound to amorphous and well-crystalline iron oxyhydroxides), f) dissolved inorganic phosphorus (DIP), g) methane (CH₄), h) sulphate (SO₄²⁻). Circles are field data, whereas lines represent model output. Note that dates are only relevant for solid phase species.

knowledging that the rate depends on both of these species and that there is a maximal rate of formation. Specifically,

$$R_{\text{viv}} = V_{\text{max}} \left(\frac{[\text{Fe}^{2+}]}{[\text{Fe}^{2+}] + K_{\text{Fe}^{2+}}} \right) \left(\frac{[\text{HPO}_4^-]}{[\text{HPO}_4^-] + K_{\text{HPO}_4^-}} \right) \quad (1)$$

where V_{max} is the maximal rate ($\text{mol L}^{-1} \text{s}^{-1}$), $K_{\text{Fe}^{2+}}$ (mol L^{-1}) and $K_{\text{HPO}_4^-}$ (mol L^{-1}) are half-saturation constants for their respective species. The choice of reaction kinetics is discussed in detail in section 4.3 below.

3.3. Boundary conditions & model solution

At the lower boundary of the model, all species employ zero-gradient boundary conditions, except where data reveals solute fluxes from depth and thus a flux is prescribed accordingly. At the upper boundary, solute concentrations are specified at the edge of the diffusive boundary layer, while sedimentation of particulate material is accounted for by prescribed fluxes (see below). A full list of the boundary conditions is included in the Supplementary Material.

Partial differential equations that describe mass balance of chemical species are solved using the Method of Lines approach (e.g., Boudreau, 1996) whereby spatial derivatives are replaced by finite difference approximations and integrated numerically with the `ode` ordinary differential equation solver (Soetaert et al., 2010). The model is written in a combination of R and C. For each simulation, the model is run to steady-state with initial forcings before transient simulations are performed. Additional details of the model are given in the Supplementary Material.

4. Results and discussion

4.1. Geochemical profiles

Fig. 3 shows pertinent sediment and pore water profiles observed at F80, previously reported by Jilbert and Slomp (2013a)

with the exception of CDB-Fe and solid phase sulphur. Below 5 cm depth, CDB-Fe and solid phase sulphur concentrations exhibit the same trends, yet differ in magnitude by a factor of ~2. While an iron speciation was not undertaken at F80, an observed S:CDB-Fe ratio of 2:1 suggests that the majority of this iron and sulphur is bound in pyrite (FeS₂), an assertion that is supported by data from analogous sites in the adjacent Gotland basin (Boesen and Postma, 1988). Above 5 cm, both CDB-Fe and Fe–P show a local maximum close to the sediment–water interface and decline with increasing depth. These data are indicative of phosphorus bound to iron oxyhydroxides that undergo dissolution during burial, as seen elsewhere in the Baltic Sea (Mort et al., 2010). Fe–P maintains a relatively constant concentration beyond the upper 5 cm, but shows a broad enrichment below 20 cm that has been putatively identified as vivianite (Jilbert and Slomp, 2013a). Nevertheless, pore waters at F80 are undersaturated with respect to vivianite due to low Fe²⁺ concentrations (Jilbert and Slomp, 2013a), implying that iron is the rate limiting substrate. Assuming second order reactions kinetics, vivianite precipitation would effectively scale linearly with iron availability. This is not evident in the data, however, as the peak in Fe–P observed at depth (Fig. 3) is much less pronounced than predicted when using second order kinetics (results not shown). These preliminary simulations suggest that at some point vivianite precipitation becomes kinetically limited, reaching a maximum rate of formation in spite of reactant concentrations, like Michaelis–Menten kinetics (see section 3.2). Furthermore, if vivianite formation is indeed microbially-mediated, as recent observations suggest (e.g., Milucka et al., 2012), equation (1) is an appropriate description of kinetics (Thullner et al., 2007). Immediately above this Fe–P enrichment, the organic carbon profile exhibits a near stepwise increase that is also evident in the organic phosphorus profile. Finally, sulphate decreases to zero with depth, whereas methane increases. The trends exhibited by the methane and sulphate profiles suggest that anaerobic oxidation of methane (AOM) is occurring (Devol, 1983).

4.2. Hypothesized scenario

Geochemical signals recorded in deep sediments, like those described above, reflect fluctuations in environmental conditions in the overlying water column and shallower sediments. These signals can thus be used to reconstruct shifts in biogeochemical dynamics in the basin due to eutrophication. The hypothesized transition into deep basin euxinia as a result of eutrophic surface waters, including temporal variations in the iron shuttle, is as follows. Elevated primary production associated with an abundance of nutrients in surface waters enhances the export of organic matter from the euphotic zone, thus increasing benthic oxygen demand and dissimilatory iron reduction in underlying sediments. In coastal regions, oxygen penetration into sediments decreases allowing Fe^{2+} to escape into the water column, where iron oxyhydroxides precipitate and are deposited deeper in the basin (Canfield et al., 1996). This mechanism concentrates iron deep in the basin and has shown to be active in the Baltic Sea (Scholz et al., 2013). Consistent with data from numerous deep sites in the Baltic Sea (Lenz et al., 2015), the iron shuttle increases to a peak before declining to a relatively constant background value in subsequent decades. In addition, the iron shuttle is accompanied by an enrichment in organic matter due to enhanced productivity in surface waters as eutrophication spreads to pelagic waters. Consequently, there is an increase in benthic oxygen demand in deep basins, which leads to hypoxia, anoxia, or sulphidic conditions.

At F80, there is a broad enrichment in Fe–P that is overlain by a large peak in solid phase sulphur, which coincides with a near stepwise increase in organic matter concentration (Fig. 3). The presence of reduced iron phosphates beneath organic matter and iron sulphide enrichments implies that pyrite formation was initially sulphide limited, because the onset of the iron shuttle preceded the marked rise in organic loading that stimulated diagenetic sulphate reduction in the deep basin. During this period, sulphate reduction in deep sediments remained relatively low due to a modest depositional flux of organic matter, meaning little hydrogen sulphide was produced. Thus, in deep basins Fe^{2+} liberated from oxyhydroxides through dissimilatory iron reduction was not subsequently bound in iron sulphides, but rather in vivianite as manifested in the broad peak in Fe–P profile (Fig. 3). As eutrophication intensified, however, export from surface waters increased resulting in an accumulation of organic matter in deep sediments and elevated sulphate reduction. Although diagenetic sulphide production increased, there was a decline in the amount of sulphide sequestered in sediments as pyrite, mackinawite, and other minerals, because less iron was deposited as the iron shuttle began to wane. This allowed for more sulphide to diffuse out of sediments and resulted in sulphidic bottom waters. As these conditions favoured the formation of iron sulphides over iron phosphates, vivianite precipitation declined. This scenario is summarised in Fig. 4.

4.3. Constraining forcing parameters and model solution

To validate the hypothesized scenario, the reactive-transport model described above was employed to simulate the proposed shifts in environmental parameters and then resulting profiles were compared against observations. Initially, the model was run to steady-state with environmental conditions from 100 yrs ago. Forcing parameters for this scenario (Fig. 5) are constrained using numerous independent observations and sediment and pore water profiles presented here. These constraints – pertaining to organic matter deposition and degradation, bottom water redox conditions, solid phase iron fluxes, and vivianite kinetics – are discussed in detail below.

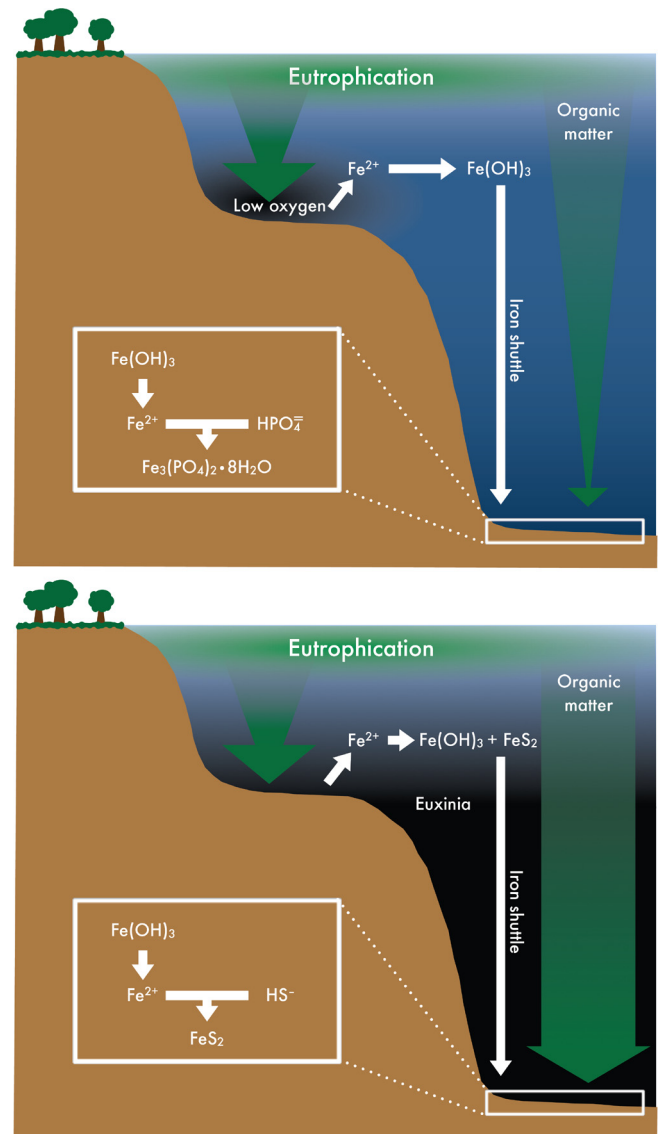


Fig. 4. A schematic of depositional and diagenetic dynamics at F80. The top pane shows the onset of the iron shuttle prior to enhanced organic matter deposition to deep sediments and resulting euxinia. Fe^{2+} liberated from oxyhydroxides in sediments is therefore incorporated into vivianite due to a dearth of hydrogen sulphide. The lower pane shows a transition into euxinia and elevated organic loading, which result in diagenetic iron sulphide formation.

Incoming organic matter is divided into three pools according to lability – the so-called multi-G approach (Berner, 1980; Westrich and Berner, 1984). Consistent with observations, organic matter that is deposited at the sediment-water interface is assumed to be 50% labile, 16% less labile, and 34% inert organic matter (Westrich and Berner, 1984), like previous studies in the Baltic Sea that used the multi-G model (Reed et al., 2011b). These pools decompose at different rates: the first is remineralised quickly, the second is slower to degrade, and the third is entirely inert. This gives rise to regions of the organic carbon profile with markedly different gradients. Specifically, the slope close to the sediment-water interface reflects decomposition of the most labile material, whereas deeper in the sediment the gradient is due to degradation of less labile organic matter (Fig. 3). Together with an age model, these gradients can be used to estimate rate constants for the various pools. Here, we used the age model for F80 previously published by Lenz et al. (2015). Estimated rate constants (Table S9) are consistent with sites that have similar sedimentation rates and

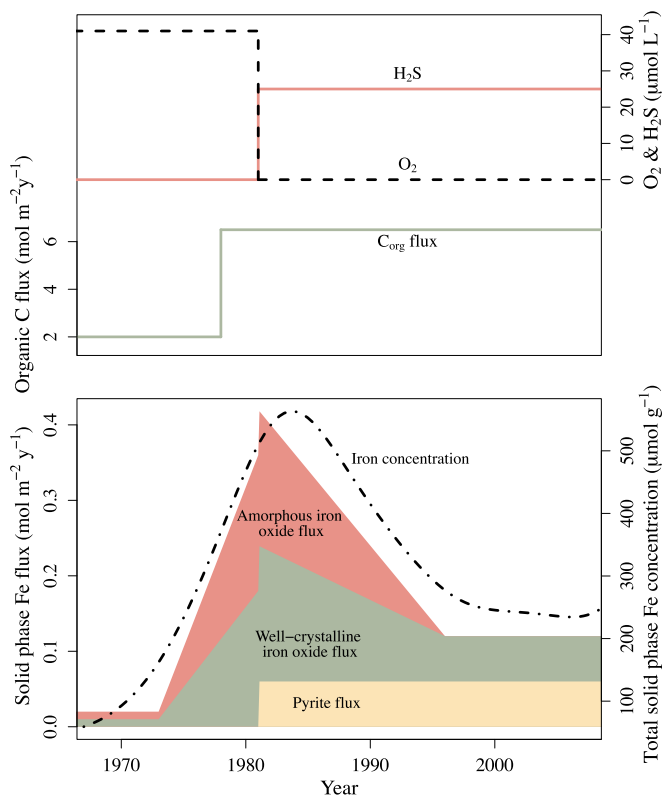


Fig. 5. Forcings used to drive the baseline model simulation over time: (top) organic loading and bottom water concentrations of oxygen and hydrogen sulphide and (bottom) the magnitude and speciation of the iron shuttle. The dashed line in the bottom pane represents the CDB iron concentration in sediments with the spatial dimension transformed into the temporal dimension using $t(x) = \int_0^x [w(\xi)]^{-1} d\xi$ where $t(x)$ is time taken for a particle to reach depth x due to burial and $w(\xi)$ is the burial velocity of solids at depth ξ .

depths (Arndt et al., 2013), although the range of observed values is quite large. The C:N:P ratio of incoming organic matter is defined according to observed the C:N:P ratio of organic matter recently deposited at the sediment surface.

Between the beginning and end of the 20th century, there was a marked increase in primary production and organic matter deposition in the Baltic Sea. Analysis of pCO₂ data from the Baltic Proper suggests that primary production has increased by a factor of 1.8–3.8 since the beginning of the last century (Schneider and Kuss, 2004). Reconstructions using basin-scale physico-biogeochemical models have yielded similar estimates. Savchuk et al. (2008) determined that productivity in the Baltic Proper rose by a factor of 3.0–3.4 over the past century, while the average annual biomass in surface waters (<10 m) was estimated by Gustafsson et al. (2012) to be elevated by a factor of 3.07 in the latter half of the 20th century relative to the beginning of the century. At site F80, this increase in organic matter production and export is manifested as a near stepwise shift in the organic carbon and phosphorus profiles around 1978 (Fig. 3). Depositional fluxes of organic matter before and after this shift were determined by choosing fluxes that produced the best fit to observations (Fig. 3). When estimated in this manner, the model predicts that organic matter loading increased by a factor of 3.25 over the 20th century, which is in good agreement with the three independent studies discussed previously.

Observations show bottom water oxygen concentrations of ~41 μM at the beginning of the 20th century before the system descended into euxinia shortly afterwards in 1981 due to the marked increase in organic loading around 1978 and an associated increase in sulphate reduction (Fig. 2; Gustafsson et al.,

2012). Accordingly, bottom water redox conditions – specifically, concentrations of oxygen and hydrogen sulphide – are specified to be consistent with these observations (Fig. 5). A feasible variant of the proposed scenario is that oxygen was lower than ~41 μM in the early 20th century, as there were few observations to constrain bottom water oxygen concentrations in the Fårö deep prior to 1960 (Fig. 2). Molybdenum measurements in both the Fårö Deep and the neighbouring Gotland basin suggest that the water column was not euxinic during this period – indeed Mo:Al ratios suggest that euxinia began around 1981, in agreement with simulations presented here (Jilbert and Slomp, 2013b; Lenz et al., 2015). Nonetheless, bottom water oxygen concentrations in the Fårö basin could have been close to zero at this time. To reconstruct observed sediment and pore water profiles when assuming anoxia prior to 1980 requires only two revisions to the hypothesized scenario. First, the peak in the iron shuttle must be increased in magnitude by 25%. The absence of oxygen at the sediment–water interface allows Fe²⁺ to escape quickly into the water column and, therefore, less iron is retained within the sediments meaning solid phase iron and sulphur profiles are underestimated. Related to this, the second necessary amendment is a 15% increase in the rate constant for vivianite formation, as iron must be bound more rapidly or be lost to bottom waters. These are very minor changes and do not alter the dynamics nor timeline of the original scenario, just the magnitude of two parameters. Indeed, vivianite precipitation and the record of the iron shuttle in sediments are shown to be quite insensitive to bottom water oxygen and hydrogen sulphide concentrations (Fig. S5).

Next, the iron shuttle is estimated by tuning the depositional flux of solid phase iron to reproduce the observed profile for CDB Fe (Fig. 3). Accordingly, the iron shuttle is assumed to increase linearly beginning in 1973 to a peak in 1981 before declining linearly again to a constant value after 1996. While there is no sediment trap data available to corroborate the timing of the peak – since iron deposition is typically not measured during monitoring programs – the sedimentary record at numerous sites throughout the Baltic Sea shows peaks in solid phase iron at approximately the same time (Lenz et al., 2015). The speciation of the iron shuttle is subject to several additional constraints. First, during the oxic phase, iron is deposited as oxyhydroxides that is divided equally between amorphous and crystalline pools (Berg et al., 2003). As the iron shuttle declines, we assume crystalline iron oxides start to dominate, as they are more resilient to dissolution in the water column. Next, a flux of oxyhydroxides was maintained during euxinia, as the observed CDB-Fe profile exhibits the familiar exponential decline from a maximum concentration at the sediment–water interface (Fig. 3), which is indicative of the presence of iron oxyhydroxides that undergo reduction during burial. Finally, at the onset of euxinia, a flux of pyrite is also prescribed reflecting that iron sulphides are stable and efficiently sequestered under anoxic conditions. Reconstructing depositional fluxes through a combination of independent constraints and sediment profiles is a powerful facet of reactive-transport modelling that has proven successful in the past (e.g. Reed et al., 2011a). Varying the timing and magnitude of the iron shuttle illustrates the sensitivity of CDB Fe to the depositional flux of iron and supports the choice of forcing function used here (Fig. S3).

Finally, parameters associated with vivianite precipitation must be constrained. Pore waters are undersaturated with respect to vivianite (Jilbert and Slomp, 2013a), which precludes the use of a standard description of (abiotic) mineral precipitation. Second order kinetics are also not applicable, as the peak at depth that is produced when adopting these kinetics is too high suggesting that a maximum rate is achieved, like that predicted by Michaelis–Menten kinetics. A recent study suggests that vivianite could be produced intracellularly (Milucka et al., 2012) supporting the use

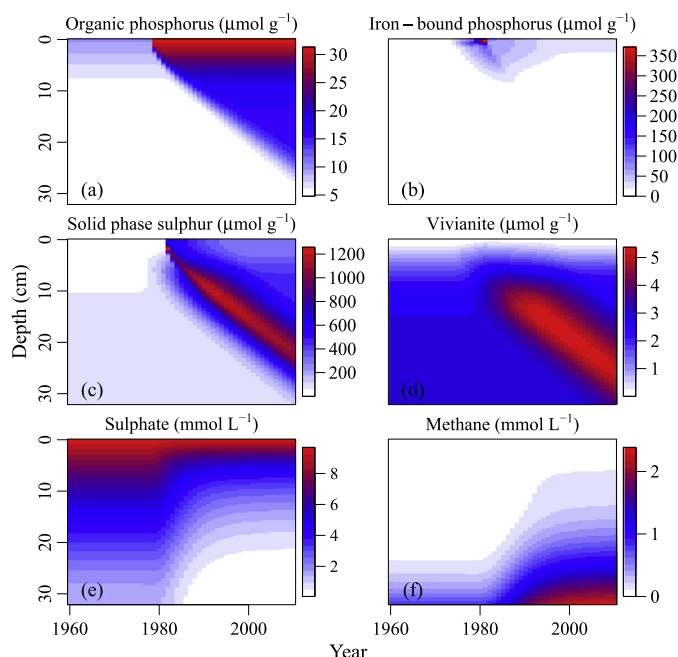


Fig. 6. The temporal evolution of relevant chemical profiles.

of Michaelis–Menten kinetics, which are often used to describe microbially-mediated geochemistry (e.g., Thullner et al., 2007). The maximum rate constant and half-saturation coefficients are chosen to reproduce observations (Fig. 3) and varying these parameters causes the model solution to deviate further from the observed iron-bound phosphorus profile (Fig. S2). While more work is needed to reveal the details of the mechanisms producing vivianite, the current approach is supported by data that is currently available.

4.4. Reconstructing the depositional and diagenetic history of F80

A major benefit of reconstructing observed profiles using a reactive-transport model is the ability to examine how sedimentary features developed in response to environmental forcings and to establish the timing of events. To this end, Fig. 6 shows the temporal evolution of chemical profiles in response to variable environmental forcing (i.e., iron deposition, organic loading, and redox conditions; Fig. 5). In addition, Fig. 7 plots the sedimentary inventories of iron and phosphorus over the past 50 yrs at F80.

Simulations show an enrichment in iron oxyhydroxides at the sediment-water interface around 1981 (Fig. 6b) coinciding with a peak in the iron shuttle (Fig. 5). The timing and form of the simulated iron shuttle is consistent with data from numerous deep basin sites in the Baltic Sea (Lenz et al., 2015). During burial, these oxyhydroxides are rapidly reduced producing Fe^{2+} that initially precipitates as vivianite in the uppermost 10 cm of sediments, in agreement with previous assertions (Jilbert and Slomp, 2013a). Shortly afterwards, however, formation of vivianite declines in favour of pyrite precipitation, which is triggered by an increase in organic loading. At this point bottom waters are still hypoxic, however, meaning these iron sulphides may still be oxidised and thus contribute to active iron cycling. In contrast, under anoxic or euxinic conditions iron sulphides are stable and consequently sequester iron. An elevated export of organic matter to sediments at F80 – which is apparent from a near stepwise shift in the organic carbon profile (Fig. 3) – causes an upward migration in the sulphate–methane transition zone (SMTZ; Fig. 6e & f) by stimulating sulphate reduction and methanogenesis. Sulphate concentrations are drawn down by dissimilatory sulphate reduc-

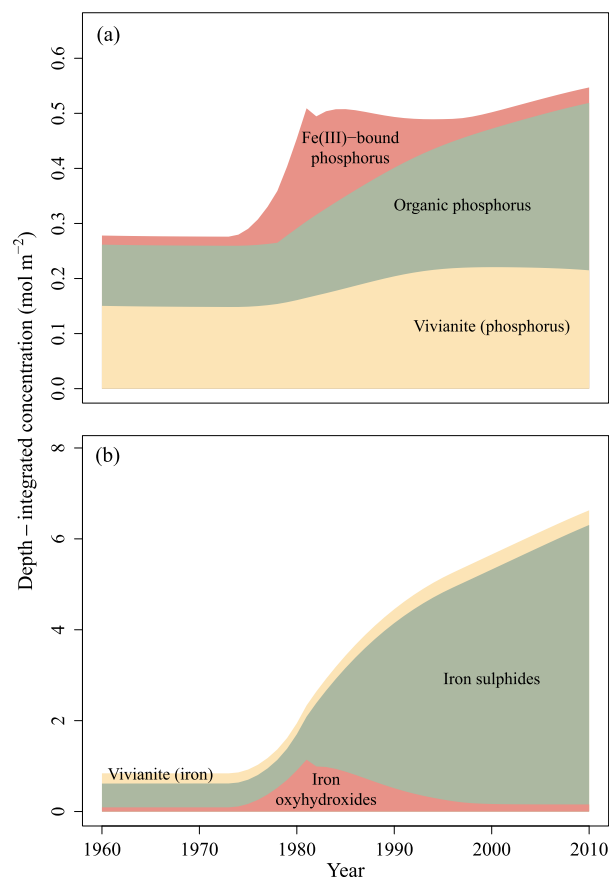


Fig. 7. Depth-integrated solid phase concentrations over time for (a) phosphorus and (b) iron.

tion and anaerobic oxidation of methane (AOM) resulting in the observed shift in the SMTZ towards the sediment-water interface. These reactions both produce hydrogen sulphide, which has a high affinity for iron, leading to an increase in iron sulphide precipitation (e.g., mackinawite, pyrite). Thus, enhanced organic matter deposition attenuates vivianite formation by limiting iron availability through this mechanism, which is manifested in the Fe–P and solid phase sulphur profiles as a broad peak in vivianite at depth overlain by a peak in pyrite (Fig. 3). Following precipitation, sulphur and vivianite enrichments associated with the peak in iron oxyhydroxide deposition are subsequently buried unaltered (Fig. 6c & d). While vivianite plays an important role in sequestering phosphorus (Fig. 7a), its contribution to the sedimentary iron budget is very minor due to the abundance of pyrite at F80 (Fig. 7b).

Organic phosphorus (P_{org}) shows a marked increase at the sediment-water interface as a result of elevated organic loading after 1978 (Fig. 6a). While there is sharp decrease in organic phosphorus from 0 to 8 cm due to the remineralisation of labile organic compounds, much of the organic matter that is deposited is subsequently buried, sequestering phosphorus as a result. P_{org} is presently the dominant phosphorus species at F80 and exhibits a linear increase with time implying it represents a growing P sink, whereas vivianite and iron-bound phosphorus have remained relatively constant in recent years (Fig. 7a). Nevertheless, this has not always been the case. As a result of the iron shuttle, iron-bound phosphorus became the dominant phosphorus species in sediments during the mid-1980s, but concentrations subsequently declined due a decrease in iron deposition and a transition into more reducing conditions (Fig. 7a). Nonetheless, this accumulation of a relatively large quantity of reactive iron stimulated vivianite formation, leading to an increase of 50% in $\text{Fe}_3(\text{PO}_4)_2 \cdot 8\text{H}_2\text{O}$

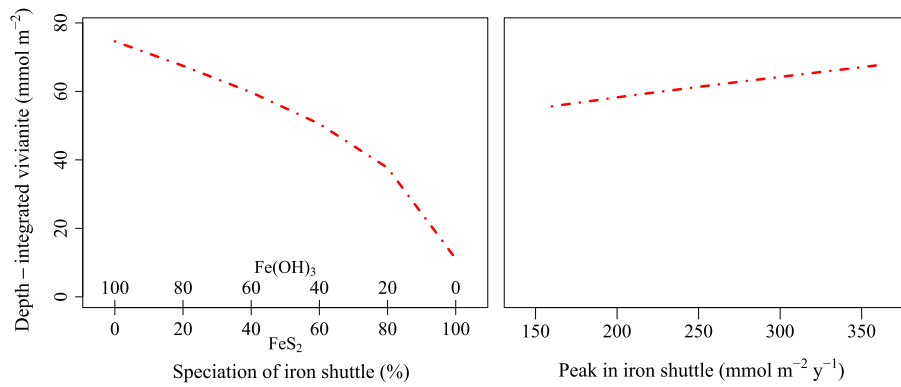


Fig. 8. Depth-integrated vivianite concentration versus (left) speciation of iron shuttle (the horizontal axis shows the percentage that is iron oxyhydroxides and pyrite) and (right) maximum value of the iron shuttle.

concentration in a matter of decades. Unlike iron oxyhydroxides, reduced iron (II) phosphates persist under anoxic conditions retaining phosphorus that would otherwise have been released to the water column and contributed to the positive feedback between anoxic bottom waters and eutrophication. This provides impetus for a quantification of the factors that control the magnitude of vivianite production and sulphidic bottom waters.

4.5. Variable Fe shuttling impacts vivianite formation & bottom water sulphide

Prior to the onset of euxinia at F80, Fe^{2+} is bound in iron (II) phosphate minerals due to a dearth of sulphide, which is manifested by a broad peak at depth in the Fe–P profile (Fig. 3e). When bottom waters become sulphidic, however, dissolved iron is rapidly bound as iron sulphides and iron (II) phosphate precipitation declines, illustrating that iron availability modulates vivianite formation. Nevertheless, iron availability is not only controlled by diagenesis, but also by deposition. Thus, we examine the impact that both the magnitude and speciation of the iron shuttle have on vivianite concentrations.

Depth-integrated vivianite concentration shows a strong correlation with the speciation of the iron shuttle (Fig. 8(left)). Little $\text{Fe}_3(\text{PO}_4)_2 \cdot 8\text{H}_2\text{O}$ is formed when the iron shuttle is primarily pyritic, as pyrite is stable under anoxic conditions and, thus, efficiently sequesters iron when deposited under euxinic bottom waters. These results indicate that vivianite is unlikely to play an important role in phosphorus dynamics after deep basins become sulphidic. Therefore, the timing of the iron shuttle relative to the onset of euxinia has important implications for phosphorus dynamics, because this determines the speciation of iron that is deposited in deep basins. In contrast, vivianite has the potential for forming in regions where the iron shuttle is active due to eutrophic surface waters, yet where deep waters remain oxic or even hypoxic, as this precludes the syngenetic formation of pyrite. Since precipitation of vivianite is limited by iron availability, the magnitude of the iron shuttle also affects the amount of $\text{Fe}_3(\text{PO}_4)_2 \cdot 8\text{H}_2\text{O}$ that is formed (Fig. 8(right)). Specifically, simulations show that the amount of vivianite found in sediments scales linearly with the depositional flux of iron. Furthermore, the magnitude of the iron shuttle also modulates water column redox conditions, as the capacity of sediments to retain sulphides is determined by iron availability. Sediments with higher depositional fluxes of iron produce more vivianite because they are able to sequester greater amounts of sulphides, thus also maintaining a non-sulphidic water column for longer. Under these conditions, there is more iron present in the sediments due to a higher flux and, in addition, it is of a form that is conducive to vivianite formation (i.e., as iron oxides).

Given the impact that the magnitude and speciation of the iron shuttle have on vivianite concentrations, it is important to be able to accurately quantify the iron shuttle. Palaeoceanography relies on numerous different proxies to reconstruct redox conditions, such as $\text{C}_{\text{org}}:\text{P}_{\text{tot}}$ (Ingall et al., 1993) and Mo (Brumsack, 1989), while bulk sedimentary iron is often used as a proxy for iron deposition (Canfield et al., 1996). To examine the utility of the latter proxy, the depositional flux of iron over time is compared to the iron concentration recorded in sediments at F80. The iron profile is transformed from a spatial to a temporal dimension using $t(x) = \int_0^x [w(\xi)]^{-1} d\xi$, where $t(x)$ is time taken for a particle to reach depth x due to burial and $w(\xi)$ is the burial velocity of solids at depth ξ . Simulations show that despite active early diagenesis (see section 4.4), the solid phase iron profile closely reproduces the depositional signal for iron (Fig. 5). The rise in Fe:Al observed prior to the onset of euxinia at F80 thus reflects elevated iron deposition due to increased down shelf iron transport (Lenz et al., 2015), which results from enhanced organic loading in coastal sediments and oxygen depletion in these regions. Similarly, the subsequent decrease in solid phase iron reflects a decline in iron export to deep sediments, likely due to the onset of sulphidic conditions in shallow waters sequestering iron as meta-stable sulphides in underlying sediments (e.g., Scholz et al., 2014). In turn, this encourages euxinic deep waters: less iron deposition means that more sulphide is able to escape from sediments into overlying waters. Thus, while trace metals (e.g., Mo, V) offer insights into local redox conditions, Fe:Al casts these insights into a broader context by providing information about regional redox dynamics (Eckert et al., 2013).

4.6. Inflow events

Deep basins within the Baltic Sea are episodically ventilated by major inflow events (Matthäus and Franck, 1992; Schinke and Matthäus, 1998; Meier, 2007), which have occurred on average once a decade in recent years. During these events, saline, oxygenated waters from the North Sea pass over the Darss Sill and sink to replace existing bottom waters due to relatively high densities (Stigebrandt, 1987). As a result, deep sediments in regions such as the Fårö basin are subject to periodic reoxygenation after which conditions decline once again (Matthäus and Franck, 1992). The water column data in Fig. 2, suggest that hydrogen sulphide-rich waters more readily developed following inflows than at the start of the modern hypoxic event. This could possibly be related to a more muted iron shuttle. Redox fluctuations also have a profound impact on benthic phosphorus cycling (Reed et al., 2011a, 2011b; Kraal et al., 2010; Tsandev et al., 2012; Ingall et al., 1993; Slomp et al., 2002; Jilbert et al., 2011), although it is unknown how such fluctuations affect vivianite precipitation. Simulations

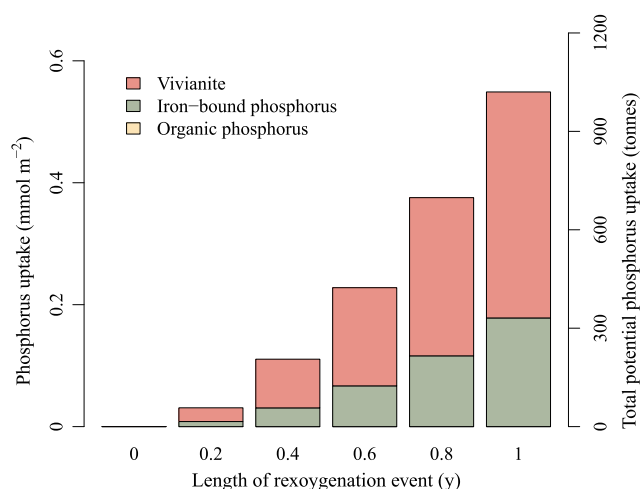


Fig. 9. Increase in sedimentary phosphorus uptake due to major inflow events. The horizontal axis shows the length of the reoxygenation events.

were undertaken to examine the impact of these oxic intervals on iron and phosphorus cycling in general, and vivianite formation in particular. The end point of the baseline scenario described above (section 4.2) was used as a start point for these simulations, which span a 5 yr interval. After the first year of the simulation, which uses present day (i.e., euxinic) conditions, bottom waters became hypoxic for a period with $[O_2]$ set as the pre-euxinia value from the baseline scenario. During this interval, the total iron deposition was maintained at present day levels, although iron currently deposited as pyrite was assumed to be deposited as amorphous iron oxyhydroxides. Following the reoxygenation event, conditions become euxinic once again until the end of the simulation.

Results of these simulations are plotted in Fig. 9, which shows the increase in phosphorus sequestration within sediments as a result of oxygenation events of different lengths ranging from 0.2 to 1 yr. As one would expect, there is no change to organic phosphorus uptake, but there is a marked increase in iron-bound phosphorus that correlates with the length of the reoxygenation events. When the water column is not sulphidic, iron is deposited exclusively as oxyhydroxides, thus explaining the relationship between duration of the event and iron-bound phosphorus content of the underlying sediment. Depth-integrated vivianite concentration exhibits the same trend, although more pronounced. As discussed above, vivianite formation is a function of iron availability and, consequently, an increase in reactive iron concentration (as opposed to relatively stable pyrite under anoxic conditions) leads to an increase in $Fe_3(PO_4)_2 \cdot 8H_2O$ formation. Nevertheless, iron oxyhydroxides are only a temporary sink for phosphorus and ultimately undergo dissolution upon burial, unlike vivianite which can persist. Thus, while vivianite may be a smaller phosphorus sink than iron oxyhydroxides when bottom waters are oxic, it represents a more important long term sink under low oxygen conditions.

To assess the regional importance of major inflow events, results are scaled for areas of the Baltic Sea that are anoxic (60,000 km², Jilbert and Slomp, 2013a). Short intervals of reoxygenation (0.2 yrs) produce a regional uptake of ~57 t of vivianite, whereas, in contrast, year long events potentially remove an additional ~1020 t of phosphorus from the water column. Modern day phosphorus loads to the Baltic Sea are approximately 36,000 t/yr (Gustafsson et al., 2012), suggesting that vivianite precipitation due to reoxygenation of deep waters could sequester up to ~3% of these annual loads. Nevertheless, estimates provided here are reliant on iron deposition to sediments, which is typically poorly constrained. Therefore, caution must be exercised when extrapolating

these results. While simulations suggest that artificial reoxygenation of deep waters would help to permanently sequester phosphorus in Baltic sediments as vivianite, the amount of phosphorus that is bound in vivianite is small in comparison to potentially mobile redox-sensitive species. Changes of up to 112,000 t of dissolved inorganic phosphorus per year have been observed in the Baltic Sea due to the dissolution of iron oxyhydroxides (Conley et al., 2009a). Superimposed against an active phosphorus pool of this magnitude, vivianite sequestration in sediments during to inflow events is quite minor. Thus, while vivianite needs to be incorporated in phosphorus budget calculations, stimulating its formation through artificial reoxygenation (see Conley et al., 2009b) does not represent a potential engineering solution to eutrophication in the Baltic Sea.

4.7. Implications for other coastal systems

For vivianite to precipitate under oxygen-depleted conditions, H_2S concentrations must remain low relative to Fe^{2+} otherwise iron-sulphides are rapidly precipitated rather than vivianite. There are several scenarios that may lead to this case.

First, pore waters and the overlying water column could be low in sulphate, such as in freshwater or estuarine environments. As a result, little sulphide is produced via sulphate reduction and iron released through iron reduction is readily combined with phosphate to form vivianite. Similarly, sulphate reduction could be limited by the availability of organic matter or methane, if sulphide is largely derived from anaerobic oxidation of methane. Another possibility for enhancing vivianite production is high depositional fluxes of iron oxyhydroxides, although at F80 these fluxes are already very high suggesting that this case is unlikely in a marine setting. The overarching principle is that sulphate reduction must be limited by either oxidant or reductant, while Fe^{2+} is readily produced via iron reduction.

To demonstrate that this leads to enhanced vivianite precipitation, we reran the baseline simulation with low sulphate concentrations (3 mM). As a consequence of limited sulphate reduction, iron-bound phosphorus concentrations increased by 153% with vivianite accounting for 77% of Fe–P in this scenario (Fig. S6). This illustrates that, while vivianite precipitation is not an important sink at our study site, it is potentially an important sink at locations with limited sulphate reduction. Estuaries represent such an environment, as they are often rich in iron while having markedly lower sulphate concentrations than seawater due to freshwater inputs. Furthermore, many estuaries, such as the St. Lawrence River estuary (Katsev et al., 2007), Neuse River estuary (Buzzelli et al., 2002), Chesapeake Bay (Testa and Kemp, 2012), are subject to hypoxia. Simulations presented here suggest that these conditions would be conducive to vivianite formation and may enhance phosphorus removal before waters discharge into the coastal ocean. That is to say, phosphorus filtering within estuaries may potentially alleviate eutrophication in shelf and slope waters. Another example of a potentially important setting for vivianite formation is the Bothnian Sea, located in the northern Baltic Sea. Here, sediments are rich in iron oxides and bottom waters are low in sulphate, and vivianite has been shown to account for ca. 45% of total P burial (Slomp et al., 2013; Egger et al., 2015a).

Vivianite may therefore be more prevalent than previously thought, but goes undetected since common analytical methods (e.g., SEDEX, Ruttenberg, 1992) typically do not resolve phosphorus species at a mineralogical level and calculations regarding saturation state may prove misleading (Jilbert and Slomp, 2013a). Employing analytical tools that provide a better resolution of phosphorus speciation may prove useful in elucidating the role of vivianite in phosphorus sequestration in estuarine and coastal sed-

iments, since simulations suggest vivianite may be an important sink in these regions.

5. Conclusions

Simulations undertaken with a reactive-transport model revealed that phosphorus and iron cycling are closely coupled in deep, euxinic sediments of the Baltic Sea and exhibit marked variability in response to fluctuations in redox conditions, iron deposition, and organic loading. The iron shuttle from shallow regions to the deep Fårö basin was dominated by oxyhydroxides and this increased input of reactive iron stimulated diagenetic vivianite formation. The amount of vivianite found in sediments is a function of the speciation and magnitude of the iron shuttle, which in part regulates the availability of dissolved iron. Fe:Al provides an excellent tool for reconstructing the iron shuttle (e.g., Lenz et al., 2015), especially when used in concert with other redox proxies that provide additional environmental context. Precipitation of iron (II) phosphates subsequently declined when dissimilatory sulphate reduction and anaerobic oxidation of methane increased – both of which are associated with elevated fluxes of organic matter to the seafloor – producing more hydrogen sulphide, which has a high affinity for Fe²⁺. Major inflow events that reoxygenate deep waters encourage the retention of iron-associated phosphorus in sediments, both within vivianite and bound to iron oxyhydroxides. Longer periods of reoxygenation lead to a greater sequestration of phosphorus in sediments. Finally, results suggest that some estuaries – by virtue of high iron inputs and low sulphate concentrations – could act as important phosphorus traps due to vivianite formation, thus alleviating eutrophication in shelf and slope environments. Nevertheless, the importance of vivianite in these environments may go unnoticed due to inadequate analytical techniques.

Acknowledgements

This research was funded by the European Research Council under the European Seventh Framework Programme for ERC Starting Grant 278364, the Netherlands Organisation for Scientific Research (NWO Vici; 865.13.005), the EU-BONUS project HYPER (FP7/2007–2013, Grant Agreement 217246), FORMAS, Sweden, and the Netherlands Earth System Science Centre (NESSC). We thank Dr. Tom Jilbert for his contribution to the data collection. We also thank Dr. Sergei Katsev and an anonymous reviewer for their comments, which greatly improved the manuscript.

Appendix A. Supplementary material

Supplementary material related to this article can be found online at <http://dx.doi.org/10.1016/j.epsl.2015.11.033>.

References

- Arndt, S., Jørgensen, B., LaRowe, D., Middelburg, J., Pancost, R., Regnier, P., 2013. Quantifying the degradation of organic matter in marine sediments: a review and synthesis. *Earth-Sci. Rev.* 123, 53–86.
- Berg, P., Rysgaard, S., Thamdrup, B., 2003. Dynamic modeling of early diagenesis and nutrient cycling. A case study in an Arctic marine sediment. *Am. J. Sci.* 303 (10).
- Berner, R., 1980. *Early Diagenesis: A Theoretical Approach*, 1st edition. Princeton University Press.
- Berner, R., 1984. Sedimentary pyrite formations: an update. *Geochim. Cosmochim. Acta* 48, 605–615.
- Boesen, C., Postma, D., 1988. Pyrite formation in anoxic environments of the Baltic. *Am. J. Sci.* 288, 575–603.
- Boudreau, B., 1996. A method-of-lines code for carbon and nutrient diagenesis in aquatic sediments. *Comput. Geosci.* 22 (5), 479–496.
- Boudreau, B., 1997. *Diagenetic Models and Their Implementation: Modelling Transport and Reactions in Aquatic Sediments*, 1st edition. Springer.
- Brumsack, H., 1989. Geochemistry of recent TOC-rich sediments from the Gulf of California and the Black Sea. *Geol. Rundsch.* 78 (3), 851–882.
- Buzzelli, C.P., Luettich Jr., R.A., Powers, S.P., Peterson, C.H., McNinch, J.E., Pinckney, J.L., Paerl, H.W., 2002. Estimating the spatial extent of bottom-water hypoxia and habitat degradation in a shallow estuary. *Mar. Ecol. Prog. Ser.* 230, 103–112.
- Canfield, D., Lyons, T., Raiswell, R., 1996. A model for iron deposition to euxinic Black Sea sediments. *Am. J. Sci.* 296, 818–834.
- Carstensen, J., Andersen, J., Conley, D., Gustafsson, B., 2014a. Deoxygenation of the Baltic Sea during the last century. *Proc. Natl. Acad. Sci. USA* 111 (15), 5628–5633.
- Carstensen, J., Conley, D., Bonsdorff, E., Gustafsson, B., Hietanen, S., Janas, U., Jilbert, T., Maximov, A., Norkko, A., Norkko, J., Reed, D., Slomp, C., Timmermann, K., Voss, M., 2014b. Hypoxia in the Baltic Sea: biogeochemical cycles, benthic fauna and management. *Ambio* 43, 26–36.
- Conley, D., Björk, S., Bonsdorff, E., Carstensen, J., Destouni, G., Gustafsson, B., Hietanen, S., Kortekaas, M., Kuosa, H., Meier, H., Müller-Karulis, B., Nordberg, K., Norkko, A., Nürnberg, G., Pitkänen, H., Rabalais, N., Rosenberg, R., Savchuk, O., Slomp, C., Voss, M., Wulff, F., Zillén, L., 2009a. Hypoxia-related processes in the Baltic Sea. *Environ. Sci. Technol.* 43 (10), 3412–3420.
- Conley, D., Bonsdorff, E., Carstensen, J., Destouni, G., Gustafsson, B., Hansson, S.-A., Rabalais, N., Voss, M., Zillén, L., 2009b. Tackling hypoxia in the Baltic Sea: is engineering a solution? *Environ. Sci. Technol.* 43, 3407–3411.
- Dale, A., Bertics, V., Treude, T., Sommer, S., Wallmann, K., 2013. Modeling benthic-pelagic nutrient exchange processes and porewater distributions in a seasonally hypoxic sediment: evidence for massive phosphate release by Beggiatoa? *Biogeochemistry* 10, 629–651.
- Devol, A., 1983. Methane oxidation rates in the anaerobic sediments of Saanich Inlet. *Limnol. Oceanogr.* 28 (4), 738–742.
- Diaz, R., Rosenberg, R., 2008. Spreading dead zones and consequences for marine ecosystems. *Science* 321, 926–929.
- Eckert, S., Brumsack, H.-J., Severmann, S., Schnetger, B., März, C., Fröllje, H., 2013. Establishment of euxinic conditions in the Holocene Black Sea. *Geology* 41, 431–434.
- egger, M., Jilbert, T., Behrends, T., Rivard, C., Slomp, C., 2015a. Vivianite is a major sink for phosphorus in methanogenic coastal surface sediments. *Geochim. Cosmochim. Acta* 169, 217–235.
- egger, M., Rasigraf, O., Sapart, C., Jilbert, T., Jetten, M., Rockmann, T., Van der Veen, C., Banda, N., Kartal, B., Ettwig, K., Slomp, C., 2015b. Iron-mediated anaerobic oxidation of methane in brackish coastal sediments. *Environ. Sci. Technol.* 49 (1), 277–283.
- Gustafsson, B., Schenk, F., Blenckner, T., Eilola, K., Meier, H., Müller-Karulis, B., Neumann, T., Ruoho-Airola, T., Savchuk, O., Zorita, E., 2012. Reconstructing the development of Baltic Sea eutrophication 1850–2006. *Ambio* 41, 534–548.
- Hearn, P., Parkhurst, D., Callender, E., 1983. Authigenic vivianite in Potomac River sediments: control by ferric oxy-hydroxides. *J. Sediment. Petrol.* 53, 165–177.
- Hofmann, A., Meysman, F., Soetaert, K., Middelburg, J., 2008. A step-by-step procedure for pH model construction in aquatic systems. *Biogeochemistry* 5, 227–251.
- Ingall, E.D., Bustin, R., Van Cappellen, P., 1993. Influence of water column anoxia on the burial and preservation of carbon and phosphorus in marine shales. *Geochim. Cosmochim. Acta* 57, 303–316.
- Ingall, E.D., Jahnke, R., 1994. Evidence for enhanced phosphorus regeneration from marine sediments overlain by oxygen depleted waters. *Geochim. Cosmochim. Acta* 58, 2571–2575.
- Jilbert, T., Slomp, C., 2013a. Iron and manganese shuttles control the formation of authigenic phosphorus minerals in the euxinic basins of the Baltic Sea. *Geochim. Cosmochim. Acta* 107, 155–169.
- Jilbert, T., Slomp, C., 2013b. Rapid high-amplitude variability in Baltic Sea hypoxia during the holocene. *Geology*.
- Jilbert, T., Slomp, C., Gustafsson, B., Boer, W., 2011. Beyond the Fe–P–redox connection: preferential regeneration of phosphorus from organic matter as a key control on Baltic Sea nutrient cycles. *Biogeochemistry* 8, 1699–1720.
- Katsev, S., Chaillou, G., Sundby, B., Mucci, A., 2007. Effects of progressive oxygen depletion on sediment diagenesis and fluxes: a model for the lower St. Lawrence River Estuary. *Limnol. Oceanogr.* 52 (6), 2555–2568.
- Katsev, S., Dittrich, M., 2013. Modeling of decadal scale phosphorus retention in lake sediment under varying redox conditions. *Ecol. Model.* 251, 246–259.
- Katsev, S., Tsandev, I., L'Heureux, I., Rancourt, D., 2006. Factors controlling long term phosphorus efflux in lake sediments: exploratory reaction-transport modeling. *Chem. Geol.* 234, 127–147.
- Kraal, P., Slomp, C.P., de Lange, G.J., 2010. Sedimentary organic carbon to phosphorus ratios as a redox proxy in quaternary records from the Mediterranean. *Chem. Geol.* 277, 167–177.
- Lenz, C., Jilbert, T., Conley, D., Wolthers, M., Slomp, C., 2015. Are recent changes in sediment manganese sequestration in the euxinic basins of the Baltic Sea linked to the expansion of hypoxia? *Biogeochemistry* 12, 4875–4894.
- Levin, L., Ekau, W., Gooday, A., Jorissen, F., Middelburg, J., Naqvi, S., Neira, C., Rabalais, N., Zhang, J., 2009. Effects of natural and human-induced hypoxia on coastal benthos. *Biogeochemistry* 6, 2063–2098.
- März, C., Hoffmann, J., Bleil, U., de Lange, G., 2008. Diagenetic changes of magnetic and geochemical signals by anaerobic methane oxidation in sediments of the Zambezi deep-sea fan (SW Indian Ocean). *Mar. Geol.* 255, 118–130.
- Matthäus, W., Franck, H., 1992. Characteristics of major Baltic inflows – statistical analysis. *Cont. Shelf Res.* 12, 1375–1400.

- Meier, H.M., 2007. Modeling the pathways and ages of inflowing salt- and freshwater in the Baltic Sea. *Estuar. Coast. Shelf Sci.* 74, 610–627.
- Milucka, J., Ferdelman, T., Polerecky, L., Franzke, D., Wegener, G., Schmid, M., Lieberwirth, I., Wagner, M., Widdel, F., Kuypers, M., 2012. Zero-valent sulphur is a key intermediate in marine methane oxidation. *Nature* 491, 541–546.
- Mohrholz, V., Naumann, M., Nausch, G., Krüger, S., Gräwe, U., 2015. Fresh oxygen for the Baltic Sea – an exceptional saline inflow after a decade of stagnation. *J. Mar. Res.* 148, 152–166.
- Moisander, P.H., Steppe, T.F., Hall, N.S., Kuparinen, J., Paerl, H.W., 2003. Variability in nitrogen and phosphorus limitation for Baltic Sea phytoplankton during nitrogen-fixing cyanobacterial blooms. *Mar. Ecol. Prog. Ser.* 262, 81–95.
- Mort, H., Slomp, C., Gustafsson, B., Andersen, T., 2010. Phosphorus recycling and burial in Baltic Sea sediments with contrasting redox conditions. *Geochim. Cosmochim. Acta* 74, 1350–1362.
- Mortimer, C.H., 1941. The exchange of dissolved substances between mud and water in lakes. *J. Ecol.* 29, 280–329.
- Nembrini, G., Capobianco, J., Viel, M., Williams, A., 1983. A Mössbauer and chemical study of the formation of vivianite in sediments of Lago Maggiore (Italy). *Geochim. Cosmochim. Acta* 47, 1459–1464.
- Rabalais, N., Cai, W.-J., Carstensen, J., Conley, D., Fry, B., Hu, X., Quiñones-Rivera, Z., Rosenberg, R., Slomp, C., Turner, R., Voss, M., Wissel, B., Zhang, J., 2014. Eutrophication-driven deoxygenation in the coastal ocean. *Oceanography* 27, 172–183.
- Raiswell, R., Canfield, D.E., 2012. The iron biogeochemical cycle past and present. *Geochim. Perspect.* 1, 1–232.
- Reed, D., Slomp, C., de Lange, G., 2011a. A quantitative reconstruction of organic matter and nutrient diagenesis in Mediterranean Sea sediments over the holocene. *Geochim. Cosmochim. Acta* 75, 5540–5558.
- Reed, D., Slomp, C., Gustafsson, B., 2011b. Sedimentary phosphorus dynamics and the evolution of bottom-water hypoxia: a coupled benthic–pelagic model of a coastal system. *Limnol. Oceanogr.* 56 (3), 1075–1092.
- Rothe, M., Frederichs, T., Eder, M., Kleeberg, A., Hupfer, M., 2014. Evidence for vivianite formation and its contribution to long-term phosphorus retention in a recent lake sediment: a novel analytical approach. *Biogeosciences* 11, 5169–5180.
- Ruttenberg, K., 1992. Development of a sequential extraction method for different forms of phosphorus in marine sediments. *Limnol. Oceanogr.* 37, 1460–1482.
- Ruttenberg, K., 2003. The global phosphorus cycle. In: Schlesinger, W.H. (Ed.), *Treatise on Geochemistry*, vol. 8. Elsevier, USA, pp. 585–643.
- Savchuk, O., 2010. Large-scale dynamics of hypoxia in the Baltic Sea. In: Yakushev, E. (Ed.), *Chemical Structure of Pelagic Redox Interfaces: Observation and Modeling*. In: *The Handbook of Environmental Chemistry*, vol. 22. Springer, Berlin, Heidelberg, pp. 137–160.
- Savchuk, O., Wulff, F., Hille, S., Humborg, C., Pollehne, F., 2008. The Baltic Sea a century ago – a reconstruction from model simulations, verified by observations. *J. Mar. Syst.* 74, 485–494.
- Schinke, H., Matthäus, W., 1998. On the causes of major Baltic inflows – an analysis of long time series. *Cont. Shelf Res.* 18, 67–97.
- Schneider, B., Kuss, J., 2004. Past and present productivity of the Baltic Sea as inferred from pCO₂ data. *Cont. Shelf Res.* 24, 1611–1622.
- Scholz, F., McManus, J., Mix, A., Hensen, C., Schneider, R., 2014. The impact of ocean deoxygenation on iron release from continental margin sediments. *Nat. Geosci.* 7, 433–437.
- Scholz, F., McManus, J., Sommer, S., 2013. The manganese and iron shuttle in a modern euxinic basin and implications for molybdenum cycling at euxinic ocean margins. *Chem. Geol.* 355, 56–68.
- Slomp, C., Epping, E., Helder, W., Van Raaphorst, W., 1996. A key role for iron-bound phosphorus in authigenic apatite formation in North Atlantic continental platform sediments. *J. Mar. Res.* 54, 1179–1205.
- Slomp, C., Mort, H., Jilbert, T., Reed, D., Gustafsson, B., Wolthers, M., 2013. Coupled dynamics of iron and phosphorus in sediments of an oligotrophic coastal basin and the impact of anaerobic oxidation of methane. *PLoS ONE* 8 (4), e62386.
- Slomp, C., Thomson, J., de Lange, G., 2002. Enhanced regeneration of phosphorus during formation of the most recent eastern Mediterranean sapropel (S1). *Geochim. Cosmochim. Acta* 66, 1171–1184.
- Soetaert, K., Herman, P., Middelburg, J., 1996. A model of early diagenetic processes from the shelf to the abyssal depths. *Geochim. Cosmochim. Acta* 60, 1019–1040.
- Soetaert, K., Petzoldt, T., Setzer, R., 2010. Solving differential equations in R: package deSolve. *J. Stat. Softw.* 33 (9).
- Stigebrandt, A., 1987. A model for the vertical circulation of the Baltic deep water. *J. Phys. Oceanogr.* 17, 1772–1785.
- Stoll, M., Bakker, K., Nobbe, G., Haese, R.R., 2001. Continuous-flow analysis of dissolved inorganic carbon content in seawater. *Anal. Chem.* 73, 4111–4116.
- Sundby, B., Gobeil, C., Silverberg, N., Mucci, A., 1992. The phosphorus cycle in coastal marine sediments. *Limnol. Oceanogr.* 37, 1129–1145.
- Testa, J.M., Kemp, W.M., 2012. Hypoxia-induced shifts in nitrogen and phosphorus cycling in Chesapeake Bay. *Limnol. Oceanogr.* 57, 835–850.
- Thullner, M., Regnier, P., Cappellen, P.V., 2007. Modeling microbially induced carbon degradation in redox-stratified subsurface environments: concepts and open questions. *Geomicrobiol. J.* 24, 139–155.
- Tsandeu, I., Reed, D.C., Slomp, C.P., 2012. Phosphorus diagenesis in deep-sea sediments: sensitivity to water column conditions and global scale implications. *Chem. Geol.* 330–331, 127–139.
- Van Cappellen, P., Wang, Y., 1996. Cycling of iron and manganese in surface sediments: a general theory for coupled transport and reaction of carbon, oxygen, nitrogen, sulfur, and manganese. *Am. J. Sci.* 296, 197–243.
- Villnäs, A., Norkko, J., Lukkari, K., Hewitt, J., Norkko, A., 2012. Consequences of increasing hypoxic disturbance on benthic communities and ecosystem functioning. *PLoS ONE* 7 (10).
- Westrich, J.T., Berner, R.A., 1984. The role of sedimentary organic matter in bacterial sulfate reduction: the G model tested. *Limnol. Oceanogr.* 29 (2), 236–249.

Further reading

- Rickard, D., Luther III, G.W., 1997. Kinetics of pyrite formation by the H₂S oxidation of iron (ii) monosulfide in aqueous solutions between 25 and 125 °C: the mechanism. *Geochim. Cosmochim. Acta* 61, 135–147.
- Wang, Y., Van Cappellen, P., 1996. A multicomponent reactive transport model of early diagenesis: application to redox cycling in coastal marine sediments. *Geochim. Cosmochim. Acta* 60, 2993–3014.